Solid-state vibrational circular dichroism for pharmaceutical purposes

Adam Sklenář,[a, b] Lucie Růžičková,[a, c] Lucie Bednárová,[a] Markéta Pazderková,[a] Argyro Chatziadi,[b] Eliška Skořepová,[b, d] Miroslav Šoóš,[b] Jakub Kaminský[a, *]

[a] *Institute of Organic Chemistry and Biochemistry of the CAS, Flemingovo nám.2, Prague, 166 10, Czech Republic*

[b] *University of Chemistry and Technology, Prague, Technická 5, Prague, 166 28, Czech Republic*

[c] *Imperial College London, Department of Life Sciences, South Kensington Campus, London SW7 2AZ, UK*

[d] *Institute of Physics of the CAS, Na Slovance 1999/2, Prague, 182 21, Czech Republic*

Abstract X-ray diffraction is commonly used in the pharmaceutical industry to determine the atomic and molecular structure of crystals. However, it is costly, sometimes time-consuming, and it requires a considerable degree of expertise. Vibrational circular dichroism (VCD) spectroscopy overcomes these drawbacks while also being highly sensitive to small changes in conformation and molecular packing in the solid phase. Here, we investigate the ability of VCD to distinguish between different crystal forms of the same molecule (polymorphs) and, thereby, identify those with the greatest pharmaceutical potential. First, we developed a universal experimental approach for obtaining reliable and reproducible solid-phase VCD spectra. Using three amino acids (serine, alanine, tyrosine) and one hydroxy acid (tartaric acid) as model pharmaceutical ingredients we investigated an effect of various experimental conditions on resulting VCD spectra. Solid samples were prepared using two techniques: (i) suspension of each model compound in oil (mulling agent); (ii) mixture of the model compound and crystalline powder (matrix) compressed into a pellet. Additionally, to achieve artifact-free results with a maximal signal-to-noise ratio, the following experimental conditions were optimized: time of spectral acquisition (0.5–3h), mulling agent (Nujol, fluorolube), pellet size (0.7 and 20 mm in diameter) and pellet matrix (KBr, KCl, CsI). Then, the optimized approach was successfully applied to distinguish three polymorphs of the antiviral drug sofosbuvir. Our results suggest that solid-state VCD represents a relatively rapid, cost-effective, and easy-to-use structural probe for the identification of crystal structures, with potential use in pharmaceutics.

* Corresponding author: kaminsky@uochb.cas.cz (Jakub Kaminský)

*Keywords:*vibrational circular dichroism, solid-state, amino acids, hydroxy acids, sofosbuvir, polymorphs

1. Introduction

In recent decades, research into solid-state chemical entities has grown in importance, with the determination of the hitherto-unknown structures of many solids proving essential in engineering,[1-3] as well as material and environmental science.[4, 5] More recently, it has become invaluable in the pharmaceutical sector where solid formulations of active pharmaceutical ingredients (APIs) represent a convenient way of drug administration. However, as the physicochemical properties of solids vary with the distinct atomic arrangement, new drugs often face issues of low solubility and, consequently, low bioavailability.[6] To obtain accurate knowledge of the structure of a given solid API and thus resolve all pharmacokinetics issues (ADME), the development of reliable analytical techniques for solid-phase structures is needed.[7]

Various technologies commonly used to analyze solid-state compounds have improved over time,[8, 9] but they retain some significant disadvantages. Thermal methods are commonly incapable of providing accurate atomistic insight into solid-state structures. X-ray diffraction (especially single-crystal XRD) measurements are time-consuming and sample preparation is often difficult.[10] Nuclear magnetic resonance spectroscopy (NMR), due to its complex instrumentation requirements, is rather expensive.

Conversely, vibrational (infrared (IR) and Raman) spectroscopy techniques are fast, relatively inexpensive, and require minimal sample preparation. Furthermore, these techniques are sensitive to the structure and conformation of solids.[11-13] They monitor vibrational motions sensitive to a particular atomic arrangement. Vibrational spectroscopy enables the detection of changes at the atomic level and, thereby, the differentiation of various crystalline forms of the API.[14, 15]

A chiral variant of IR spectroscopy is vibrational circular dichroism (VCD). This chiroptical method measures differences in the IR absorption of left- and right-circularly polarized light. It has extreme sensitivity to changes in the conformation and absolute structure of chiral molecules.[16, 17] Although VCD has been routinely utilized in the determination of absolute configuration in solutions, the use of VCD for solid-state analysis (ssVCD) has, thus far, been reported only recently.[3, 18-23] This is mainly because liquids provide an easy-to-measure ideal isotropic environment. On the other hand, natural anisotropy of the solid-phase results in various artifacts in ssVCD spectra,[24, 25] which must be adequately resolved for a reliable analysis. Consequently, effective ssVCD remains a challenging task, particularly in terms of reproducibility and reliability of recorded spectra.

Here, we develop a cost-effective and universal experimental procedure for the use of ssVCD in characterization of solid-state substances and even their higher-order crystal conformations. By thoroughly investigating various issues that influence the quality of recorded ssVCD, we identify the optimal approach and test it on samples of three amino acids and one hydroxy acid. Our approach is then applied to distinguish between three polymorphs of the antiviral drug sofosbuvir.

2. Materials and methods

Enantiomers of the model compounds (alanine, tyrosine, serine, and tartaric acid), mulling agents (Nujol, fluorolube), and inert matrix CsI, were purchased from Sigma Aldrich, KBr and KCl from Suprapur. Sofosbuvir was kindly provided by Zentiva k.s. and all its three studied polymorphs were prepared as described by Chatziadi et al. Ref. [26] and labelled as form 1, 6, and 7, or alternatively as form 1, A, and B in Ref. [27]

2.1. Sample preparation

The solid samples of model compounds were prepared using two techniques: (i) compressing a mixture of the studied compound and crystalline powder (matrix) into a pellet (ii) forming a suspension of the studied compound in oil (mulling agent). In the first approach, we prepared pellets by mixing the analyte with an inert matrix (KBr, CsI, KCl) in a ratio of approximately 1:100. The ratio was adjusted to obtain 0.8-1.0 absorbance of the strongest IR bands in the studied spectral region. We ground the mixture in an agate mortar or by a mill (NARVA Vibrator DDR-GM9458) and then pressurized it into a thin transparent pellet using either a laboratory hydraulic press Specac Mini Pellet Press (pellets with 7 mm diameter) or a hydraulic press Dezimalpresse DP 36 (~200 kp/cm^2) (pellets with 20 mm diameter).

In the second approach, ca 100 mg of sample was ground for 3 min in an agate mortar using a pestle until the material appeared glassy. Then, using a Pasteur pipette, four drops of mulling agent (fluorolube, Nujol) were added and mixed by the pestle to form a paste. The paste was carefully transferred using a spatula onto an optical window (BaF_2 and KBr) and covered by the second window. In hand, by gently pressing the glass plates together while rotating them in opposite directions, an even spread was assured. Amount of the paste was adjusted so that the IR absorbance of the strongest IR band was 0.8-1.0 in the spectral region of interest.

2.2. VCD experiment

All spectra were obtained using a Chiral*IR*-2X™ spectrometer (BioTools, Inc., U.S.A.) equipped with a dual-PEM™ system using two ZnSe photoelastic modulators (36.996 and 37.02 kHz, Hinds Instruments, Inc., U.S.A.) and a rotating cell (~0.3 rad.s^{-1} along the axis of incident light) allowing simultaneous recording of IR absorption and VCD. In general, the spectra were recorded at room temperature with

spectral resolution of 4 cm^{-1}, Blackman-Harris apodization function and PEM settings of 1400 cm^{-1} optimized for the mid-IR fingerprint region. Final spectra were created as an average of *N* recorded blocks; each block consisting of 1560 scans. Spectral treatment included the spectra subtraction of the corresponding matrices (measured using the identical parameters). All spectra are shown within the 1800-800 cm^{-1} spectral region. The C-H stretching vibrations in the region around 3000 cm^{-1} are beyond the scope of this study and consequently are not discussed. Using D-alanine as a model compound, the following experimental conditions were varied and their effect evaluated: 1) recording time, 2) matrix material for pellet, 3) pellet size, 4) mulling agent, 5) sampling technique (mulls or pellets).

IR and VCD spectra of the model substances as well as all sofosbuvir polymorphs were recorded in a larger (20 mm) KBr pellets using 6 scanning blocks. The IR spectra were then normalized to the most intense signals (~1620 cm^{-1}) in the amide I region. VCD signals were adjusted using the same normalization factors as the corresponding IR spectra.

2.3. Raman microscopy

Raman maps of KBr, KCl and CsI pellets with D-alanine were recorded using a confocal Raman microscope alpha300 R by WITec equipped with a high-sensitivity CCD detector, an XYZ-motorized stage and a 532 nm excitation diode laser. The pellets were mapped using a Zeiss EC Epiplan-Neofluar Dic 100×/0.9 objective. All maps (image scans) were performed for selected 50 × 50 μm regions and consisted of 28 900 points (170 × 170 spectra). The integration time for a spectrum was 0.3 s with the laser power of 21 mW, and the used grating was 600 g/mm. Total duration time of a scan was ~3 h. A sum filter calculating the overall intensity of the selected range (3000±200 cm^{-1}) was applied to process the maps to visualize the presence of studied compound in a pellet. As the presence probe we picked intense vibrations from the CH stretching region of alanine (see **Figure 4**). The intensity of the blue colour reflects the intensity of the Raman signal in that area. Cosmic ray removal and polynomial baseline correction were performed using the standard procedure in WITec Project Five software (Version 5.3.13).

2.4. Calculations

The X-ray unit cell structures of all three sofosbuvir polymorphs (CCDC Entry: CUZROG01, CUZROG02, CUZROG03) were optimized as fully periodic systems in the CASTEP program.[11] Core electrons were described by OTFG ultrasoft pseudopotentials. Valence electrons were described using plane waves with plane-wave basis-set energy cut-off of 630 eV and the ultrafine SCF tolerance. The optimization was performed at the DFT level using PBE functional[28] with semi-empirical dispersion correction (G06 correction scheme by Grimme[29]). Fine k-point

set-up (1×2×1) was employed to sample the Brillouin zone via a Monkhorst–Pack grid.[30] Lattice parameters and symmetry were fixed during the optimization and only atomic positions were relaxed. Final calculated enthalpies were normalized to the number of sofosbuvir molecules in the unit cell and related to the lowest value in the series.

Additionally, structures containing two optimized unit cells in different a, b, and c directions were systematically constructed (i.e. 2×1×1, 1×2×1, 1×1×2). Single-point energies of these structures were then calculated at the wB97X-V/6-31+G**/cosmo(water) level in Jaguar.[31] Calculated energies were then used to estimate the crystal elongation energies in each direction as: $E_{\text{elongation}} = E_{(2\times1\times1)} - 2 \cdot E_{(1\times1\times1)}$, where $E_{(1\times1\times1)}$ is the energy of a single unit cell.

2.5. Sofosbuvir characterization

The absolute configuration at the chiral centre of sofosbuvir (phosphorus atom) is the same in all three forms. Form 1 is conformationally more distinct from forms 6 and 7. Although forms 6 and 7 are conformationally similar, free rotation around a single bond allows the relative dislocation of the isopropylester group denoted as 2 in **Figure 1** with respect to the rest of the molecule. Form 1 crystallizes in a monoclinic lattice ($P2_1$ space group) containing four molecules in its unit cell. Although conformational packing and non-covalent hydrogen bonding interactions cooperate and stabilize the whole crystal structure, form 1 is the most unstable and transforms easily to other forms [26]. Form 6 has an orthorhombic system ($P2_12_12_1$ space group) with four molecules in a single elementary cell. In this form, the intermolecular interactions create rigid molecular stacks connected strongly with zigzag H-bonds. Experimentally, form 6 has been found the most compact and stable polymorph.[26] Form 7 crystallizes in a monoclinic lattice ($P2_1$ space group) like form 1, but has only two molecules in the elementary cell. Its stacking arrangement is similar as in form 6. Previously estimated energy framework (by a simplified method in CrystalExplorer[32]) revealed weaker interaction between molecular layers in form 7 than form 6, which makes form 7 less stable.[26]

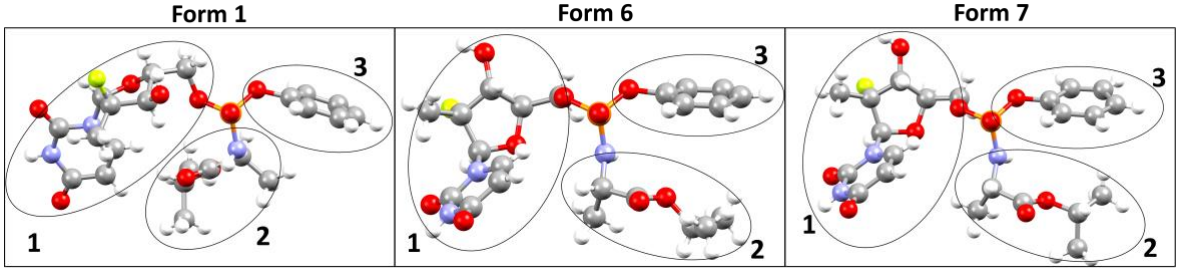

Figure 1. Three polymorphs of sofosbuvir with distinct manner of crystal packing indicated.

3. Results

3.1. Experimental procedure for ssVCD

Different sampling technique and some recommendations for ssVCD experiments have been already introduced.[33] However, no comprehensive and universal procedure for recording reliable VCD spectra of solid samples has yet been established estimating the effect of various experimental conditions on resulting spectra. Therefore, we will discuss various parameters of measurement that were accounted for to set up an optimal experimental protocol for ssVCD.

We paid special attention to artifact reduction. Common artifacts arise mostly from anisotropy of the solid-state sample, uneven distribution of particles, and their size.[34] Other sources of artifacts include different refractive indices of the sample, matrix or mulling agent, which may lead to birefringence and consequently significant linear dichroism. For that reason, we tested different sample preparation techniques (pellets or mulls) and related experimental conditions (matrix material, mulling oil, etc.). We performed testing experiments for D-alanine. **Figure S1** and **Table S1** in Supporting Information (SI) show the complete band assignment of D-alanine spectra. The quality and reproducibility of ssVCD spectra of enantiomers were later inspected using both enantiomers of alanine (see section 3.2).

3.1.1. Artifacts

Rotating the sample (the pellet or the cell with a mull) along the axis of incident light should remove artifacts originating from inhomogeneity of the distribution of studied compounds within the sample. **Figure S2** in SI shows a comparison of the VCD and IR spectra of D-alanine obtained with and without sample rotation. Static spectra were recorded for different orientations of the 7 mm KBr pellet, which were achieved by rotating it (by 0, 90, 180, and 270 degrees) in a plane perpendicular to the incident beam. The spectra of the manually rotated sample were then averaged and compared with the spectrum obtained with continuously rotated sample using the rotating cell. We see that rotation effectively replaces tedious averaging of individual orientations observable in VCD spectra. On the other hand, IR spectra are not influenced by sample rotation. Moreover, we tested flipping the sample along the axis perpendicular to the light beam. **Figure S3** in SI reveals no significant effect of such flipping, which indicates sufficient isotropy of our larger pellets. The spectra are stable in the range of 1800-800 cm^{-1}.

3.1.2. Recording time

Time may be a limiting factor for the practical utilization of a technique in real industrial operation. Therefore, we monitored the time evolution of the quality of ssVCD spectra. We inspected ssVCD spectra of D-alanine recorded using KBr pellets

for different number of blocks N (N=1 to 6) summed blocks, each consisting of 1560 scans. We used pellets of two different sizes (ø ~ 7 mm and 20 mm). One block lasted approximately half an hour and the longest experiment took ~3 hours.

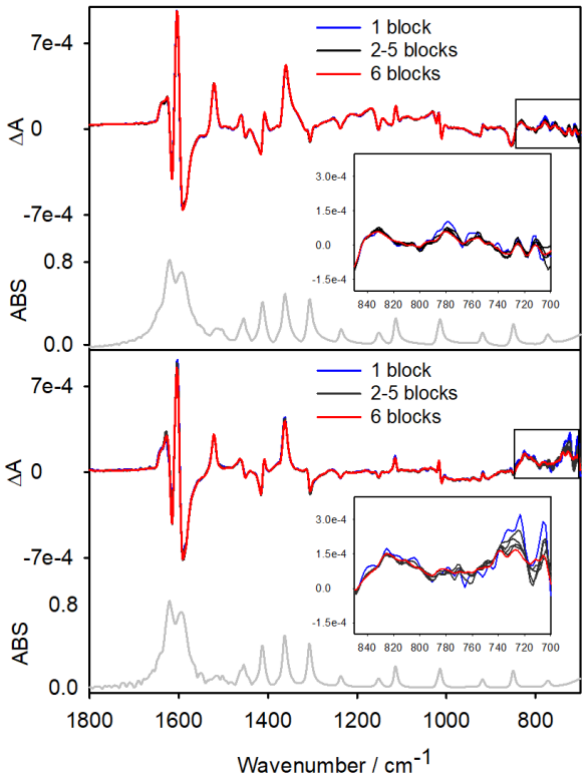

Figure 2. The effect of the number of spectral blocks (and recording time) on ssVCD spectra of D-alanine. Spectra were recorded in the larger KBr pellet (20 mm diameter; top), as well as in the smaller pellet (7 mm diameter; bottom). IR spectra (grey line) for each pellet are also presented.

Figure 2 shows a comparison of VCD spectra recorded with a different number of blocks. Spectra obtained with the 20mm pellet reveal spectral stability to ~800 cm^{-1} already for N=2 and three-hour recording (6 blocks) provides converged high-quality spectra with both pellets. However, all the spectral characteristics in the region of 1800-1000 cm^{-1} for both type of pellets are well resolved already after two blocks. Although, the observed time evolution of ssVCD spectra may be system-dependent, experiments with 2-6 blocks worked well for all solid-state samples studied in this work (alanine, serine, tyrosine, tartaric acid, and sofosbuvir). Therefore, we recommend them as a good starting point for any other ssVCD experiment.

3.1.3. Pellet materials

In this section, we focus on the eventual spectral differences due to the use of different pellet matrix materials. The pellets of 7 mm diameter with D-alanine were prepared using three alkali halides (KBr, KCl, CsI) (see **Methods** for details) and their IR and VCD spectra (**Figure 3)** were compared. **Figure S4** shows the IR and VCD spectra of the pure matrices recorded under the same conditions as for D-alanine. The

figure confirms the applicability of all matrices in the region 1800-900 cm^{-1}. As shown in **Figure 3**, we observed only minor differences between pellets of D-alanine prepared with different matrices in the range of 1800-900 cm^{-1}. Samples with all matrices provide comparable ssVCD spectra with all bands well discernible, same spectral patterns and similar relative intensities.

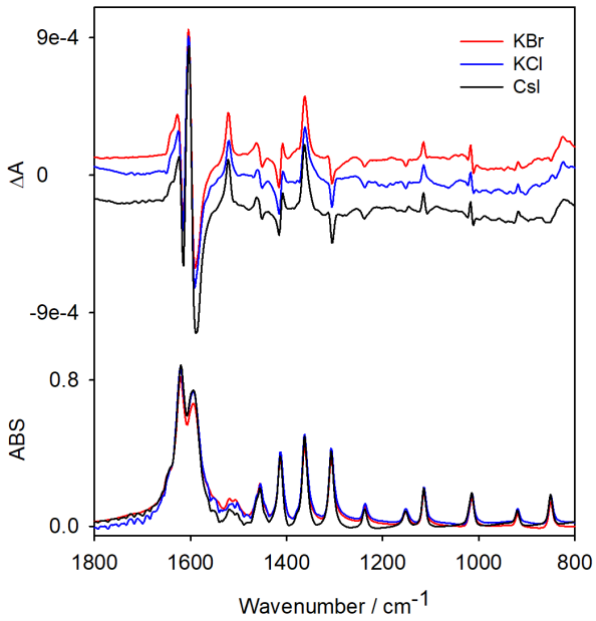

Figure 3. Comparison of D-alanine ssVCD (top) and IR (bottom) spectra measured in the 7mm pellets (7 mm diameter) prepared using three different matrix materials.

We thoroughly examined prepared KBr and CsI pellets by Raman microscopy. **Figure 4** shows Raman maps for both pellets with D-alanine. The blue regions represent areas with a significant presence of alanine. Raman mapping of pellet surfaces in **Figure 4** indicate that distribution of analyte in the KBr and CsI matrix, as well as the size of alanine crystalline particles, is comparable for both matrices. Typical size of alanine crystalline particles is of about 1 - 3 μm. Note that the average size of a crystal unit cell of D-alanine is small enough (e.g., 6.0×12.3×5.8 Å; deposition number 1102380 in CCDC) to ensure sufficient replication (~1000× in the c axis) of unit cells within the particle. This enables us to obtain the required enhancement of the VCD signal attributed to conformational consistency, native molecular ordering in crystal, and coherent delocalization of periodically stacked atoms.[35, 36] However, due to larger refractive index (RI) of CsI (RI = 1.74) in comparison to KBr (RI = 1.53) and KCl (RI = 1.44), higher price of CsI, and its high hygroscopicity, the use of CsI is not recommended.

The larger blue areas on maps in **Figure 4** are probably clusters of crystalline particles resulting from imperfect homogenization of the sample in the agate mortar. Nevertheless, the inhomogeneity of the sample distribution in the matrix or the crystal

size distribution does not negatively affect the resulting VCD spectra (see section 3.2 on reproducibility).

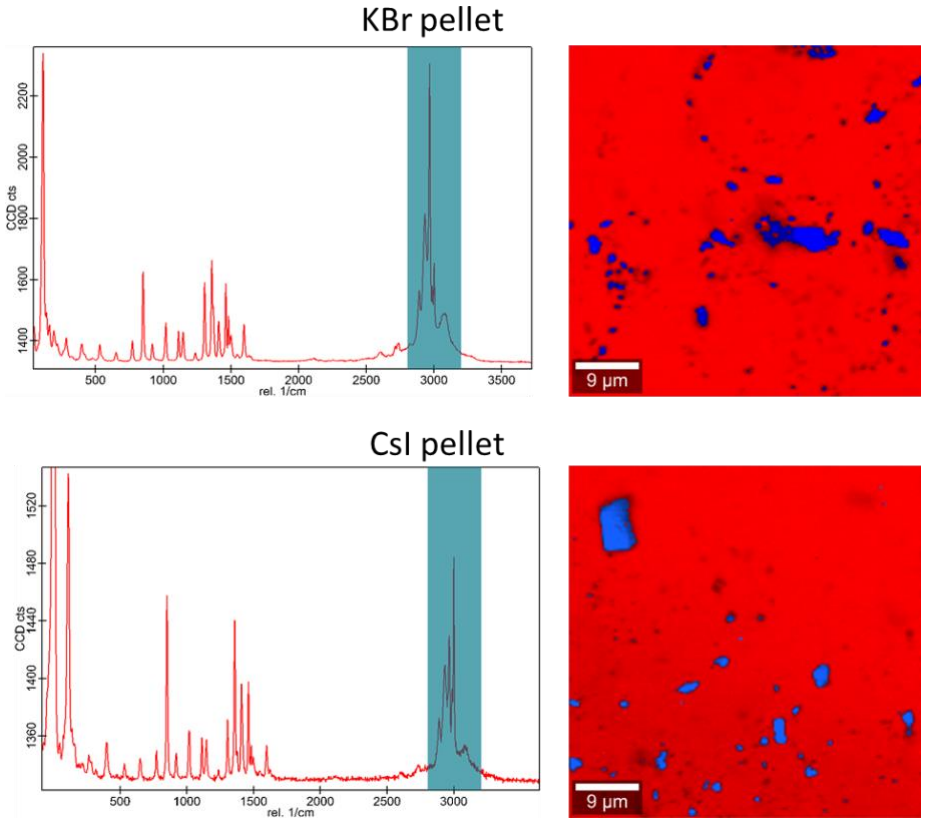

Figure 4. Monitoring the distribution of D-alanine in KBr (top) and CsI (bottom) pellets using Raman mapping. The Raman spectra on the left were taken from a region with high alanine concentration (blue regions on the right) for the demonstration. A sum filter for the range 3000±200 cm^{-1} (the blue-green marked part of the spectra; CH stretching region) was applied to visualize the presence of alanine in a pellet. Before pressing the pellets, the matrix/D-alanine mixtures were ground using an agate mortar and pestle.

3.1.4. Pellet size (KBr)

We investigated also the pellet size effect on VCD experiments. For this purpose, pellets with a diameter of ~7 mm and ~20 mm were tested. In **Figure 5**, an overlay of the spectra of D-alanine obtained using 7mm (blue) and 20mm (red) KBr pellet is shown. Except for the pellet size, the same experimental settings were used.

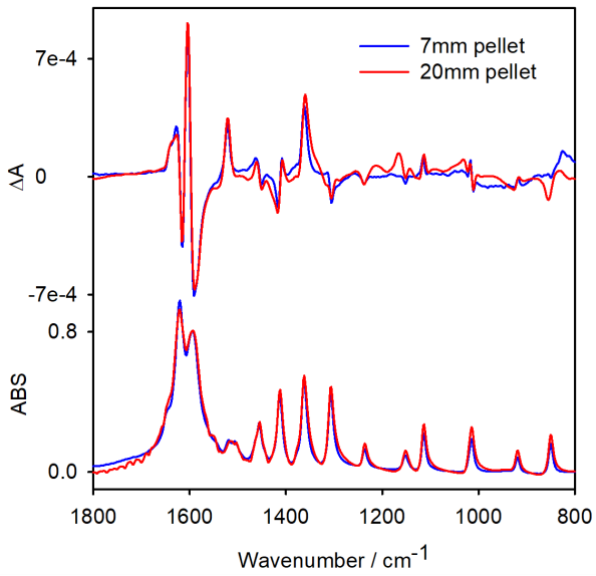

Figure 5. Comparison of ssVCD (top) and IR (bottom) spectra of D-alanine obtained using KBr pellets of different diameters.

While the IR spectra of both types of pellets resemble each other in the whole spectral range, for VCD the reproducibility is sufficient only in the region above ~900 cm^{-1}. In general, the 7mm pellet is more affected by noise and to distinguish between true signal and artifacts is rather difficult (see **Figure S5**). Thus, below 900 cm^{-1}, the quality of VCD for the 7mm pellet decreases. To get better signal quality in the low wavenumber region (1250 – 700 cm^{-1}) we prepared 7 mm pellet with a higher analyte concentration (so that the absorption of the most intense IR bands in this region was ~0.8, see **Figure S6** in SI), and recorded their VCD spectra. For this setup we observe well-distinguishable VCD signals even for this type of pellet at lower wavenumbers and 823 cm^{-1} band was confirmed to be a low concentration artifact. In case of the 7mm pellet, a significant part of the incident light is blocked by the metal ring, because its hole diameter is smaller than the beam width (~20 mm). Furthermore, pathlength of this pellet is larger than for the 20mm diameter pellet because of different pressure used for their preparation. These facts lead to an increase of offset of the absorption signal for the 7mm pellet. Thus, with the same amount of analyte the 20 mm pellet is more suitable for VCD measurements.

3.1.5. Mulling agent type (Nujol, fluorolube)

As an alternative to pellets, we also measured VCD spectra of D-alanine in suspension with mineral oils – nujol and fluorobe. Nujol exhibits two intense bands at 1460 and 1375 cm^{-1} ($\delta(CH_2)$ δ (CH_3). While nujol is suitable for the spectral region above ~900 cm^{-1}; fluorolube is applicable only for higher wavenumbers because it strongly absorbs below 1300 cm^{-1} due to $\nu(CF_2)$ and (νCF_3) vibration (**Figure 6**, middle panel). The broad band at ~900 cm^{-1} in IR spectra is due to the cut-off of BaF_2 windows

used for the measurements. Although both mulling agents are achiral (see also **Figure S4**), they increase noise in VCD spectra, which results in the loss of spectral quality. Based on these issues, we suggest either using nujol over fluorolube for ssVCD, or spectra for both oils may be joined in one final spectrum as depicted in **Figure 6**. Despite this obstacle, after subtracting signals of pure mulling agents, we acquire the VCD spectrum of D-alanine with well-resolved bands in the spectral region of 1800-900 cm^{-1}.

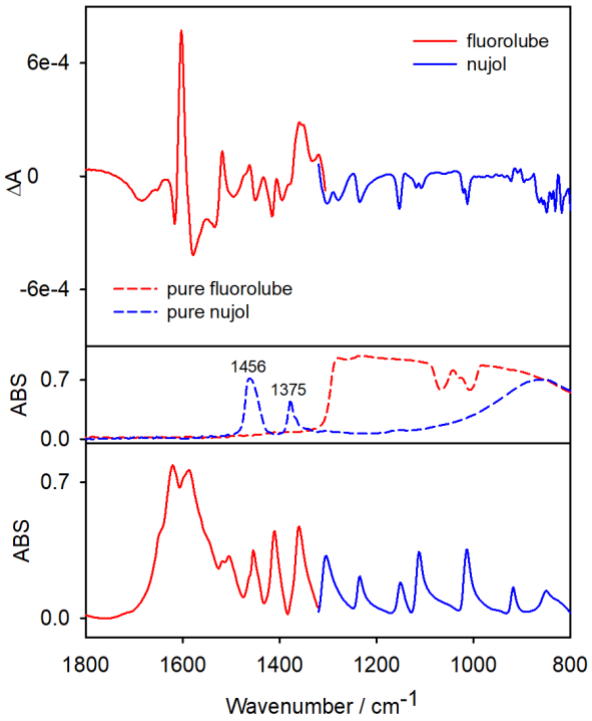

Figure 6. Joined IR (bottom panel) and VCD (top) spectra of D-alanine recorded as fluorolube and nujol mulls. The middle panel shows IR absorption of pure mulling agents.

One may argue that spectra from Figure 6 were obtained using BaF_2 windows, whereas KBr windows would be a better option, as KBr has an excellent transmission range between 40 000-400 cm^{-1}. The reason is our goal to utilize ssVCD in the pharmaceutical industry, where it would be more advantageous to use the more resilient BaF_2 than hygroscopic KBr. To demonstrate the reasonable applicability of BaF_2 windows, we compared the IR and VCD spectra of the nujol suspension of D-alanine in BaF2 windows with the same sample in KBr windows. In **Figure 7**, it is apparent that KBr optical widows provide slightly better-structured spectrum (1600-1400 cm^{-1}). Nevertheless, we obtained very well resolved bands in most of the spectral range of our interest (1800-900 cm^{-1}) with reasonable intensity even for BaF_2. As expected, the high hygroscopicity of KBr makes sample preparation and handling difficult, making this method impractical for routine industrial use.

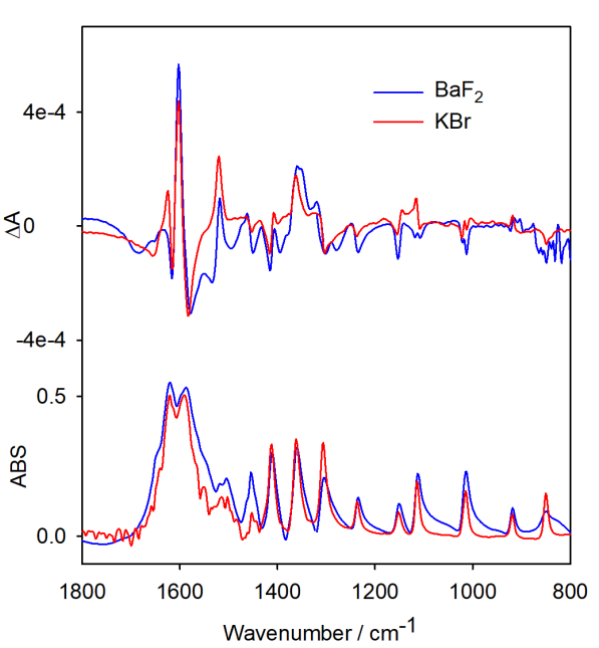

Figure 7. Comparison of solid-state IR (bottom) and VCD (top) spectra of D-alanine recorded using different optical windows.

3.1.6. Pellets versus mulls (KBr vs Nujol)

Figure 8 compares the VCD spectra obtained using both the KBr pellet and the Nujol mull placed in the KBr optical windows. As expected, we observe comparable VCD and IR spectra. The major difference in the intensity was observed at 1456 cm^{-1}, where also the Nujol mull spectrum has strong absorption due to the deformation CH_2 vibration ($\delta(CH_2)$) . Interestingly, the shape of carbonyl vibration band (1620 cm^{-1}) is rather different, which might be caused by the mechanical pressure applied during pellet preparation.

However, for further experiments we decided to use the pellet technique for the following reasons: (*i*) oil absorption interferes with the IR spectrum and increases VCD noise; (*ii*) concentration adjustment is easier and faster for pellets (iii) analyte consumption is lower for pellets; (i*v*) sample preparation of the suspension is more laborious than pellet preparation.

For the KBr pellet we also tested the effect of a different grinding technique. Two 7mm pellets were prepared by using either an automatic vibrational mill or a pestle and mortar and both were pressurized by Specac Mini Pellet Press. Spectra of both measurements are presented in **Figure S7** in SI. No significant differences in the spectra were observed, suggesting that the grinding had no effect on the resulting VCD.

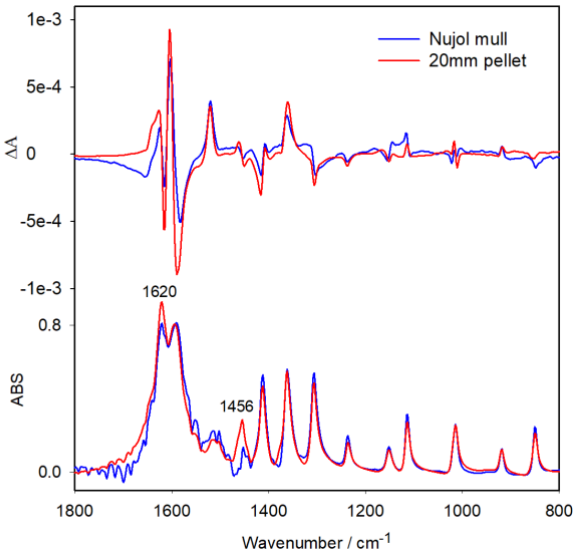

Figure 8. Comparison of IR (bottom) and ssVCD (top) spectra of D-alanine recorded using the 20mm pellet with KBr matrix and the Nujol suspension in KBr windows.

3.2. Enantiomers and reproducibility

Here we present the final spectra obtained from all previous experimentation and optimization: 20mm pellet, KBr matrix, vibrational mill. **Figure 9** shows mirror-image VCD spectra of alanine enantiomers with corresponding IR spectra. Our procedure is optimal for studying enantiomers by ssVCD in the range of ~1800-750 cm^{-1}, which is a wider range than reported so far. Using the same experimental model, but for the 7mm pellet, we also tested the reproducibility of our recorded ssVCD spectra by measuring five individually prepared samples (**Figure S8**). We can see stable and reproducible spectra.

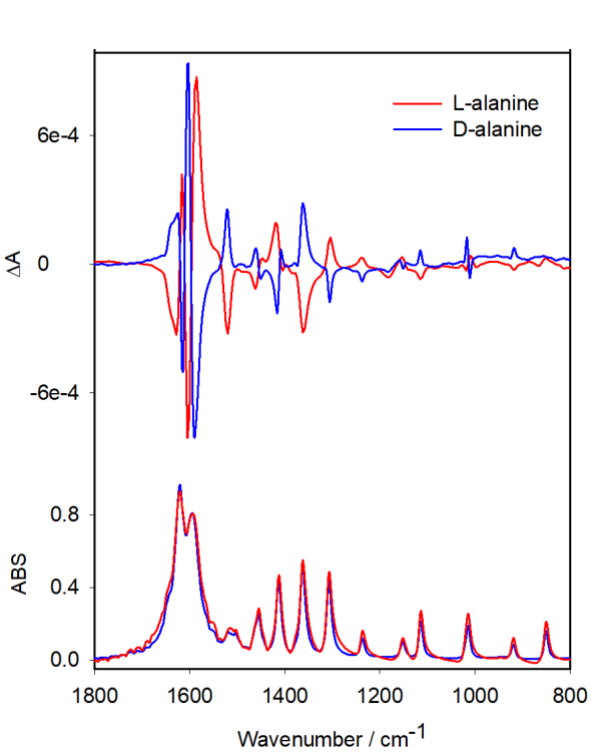

Figure 9. Solid-state VCD (top) and IR (bottom) spectra of both enantiomers of alanine recorded using the 20 mm diameter KBr pellets.

3.3. Model compounds

We apply this optimized approach for ssVCD to other model compounds (serine, tyrosine, and tartaric acid enantiomers). The samples were prepared according to same protocol as used for L- and D-alanine in 3.2.

Figure 10 shows the results for all six model compounds. Although there are a few unrealistic spectral features, such as bands at ~820 cm^{-1} in the serine or ~1310 cm^{-1} in the tyrosine ssVCD spectra, VCD patterns very well meet the general specification of a good-quality spectrum. According to our results, we can distinguish and assign most signals to vibrations as well as signal splitting. Even though tyrosine is structurally the most complicated molecule, we observe that all the VCD features are well reproduced for both strong and weak signals. If a higher resolution of relatively lower absorbance bands is needed, it is necessary to focus on the given area while increasing the analyte concentration.

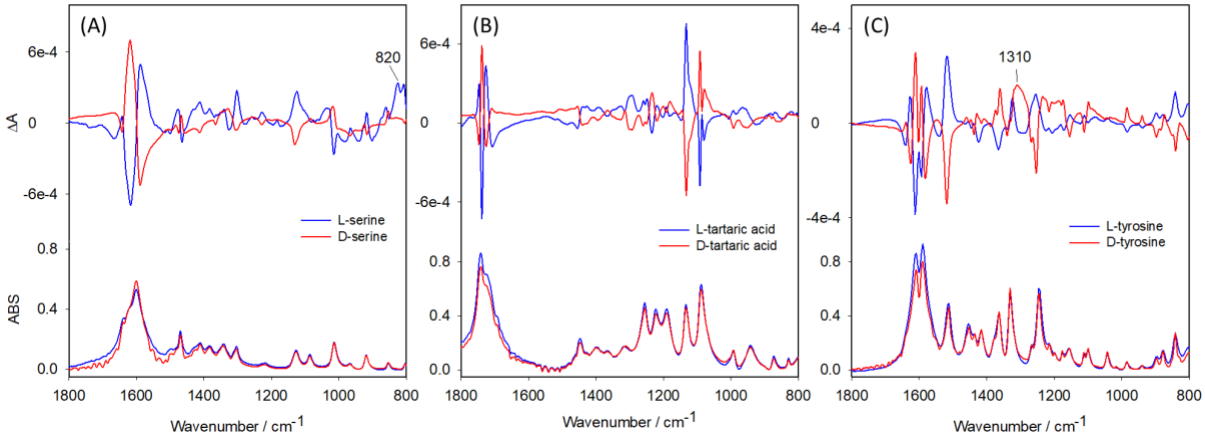

Figure 10. Solid-state VCD (top) and IR (bottom) spectra of both enantiomers of serine (A), tyrosine (B), and tartaric acid (C) recorded using the 20 mm diameter KBr pellets.

3.4. Polymorphs of sofosbuvir

Spectra of sofosbuvir polymorphs were recorded in 20 mm KBr pellets, as well as in 7 mm pellets as a control measurement (see **Figure S9**). The IR spectra of all three studied polymorphs of sofosbuvir (**Figure 11**) exhibit only a few minor differences. Specifically, the splitting in the amide I region (~1700 cm^{-1}) in form 1 is not as significant as it appears in the other two polymorphs. On the other hand, the VCD signals of this region are much more distinct in terms of both intensity and spectral patterns. Form 1 exhibits a -/+/-/+ pattern in amide I region, the opposite to forms 6 and 7. The spectral pattern of form 7 is very similar to form 6 but in overall spectrum but the signals are at the same concentration twice as intense as the signals of form 6. Also the other significant differences could be observed in the fingerprint region; form 1 has a pronounced +/- band at 1380 cm^{-1} contrary to forms 6 and 7. On the other hand, form 1 exhibits only one peak in the region between 1260 – 1210 cm^{-1} (see the blue marked region in **Figure 11**), whereas forms 6 and 7 have more complex patterns. We see another characteristic region at ~945 cm^{-1}, where forms 1 and 7 have +/- and -/+ signals, respectively. However, this band is missing in form 6.

The weaker intensity of form 6 VCD compared to form 7 cannot be simply explained by its stability, as form 6 was previously determined (both experimentally and computationally) as the most stable form.[26] Interactions between sofosbuvir layers were estimated stronger for form 6 than form 7.[26] However, the computational determination of the stability of the polymorphs was based on relatively simplified estimates of the interaction energies. These were calculated based on a single molecular wave function obtained for sofosbuvir followed by fitting the interactions between surrounding molecules to the dispersion-corrected DFT energies for the test set.[26] We decided to calculate energies (enthalpies) for all forms fully at the DFT level (see Methods for details). These are summarized in **Table S2**, where they are shown as relative energies related to form 7 and normalized to the number of

sofosbuvir molecules in the cell. The enthalpy relates to the lattice energy dissimilarities between different forms and thus reflects the structure and mutual interactions of molecules within the unit cell rather than larger interaction patterns between molecular layers and cells. **Table S2** in SI reveals that form 7 has the lowest lattice energy followed by form 1 (1.41 kcal/mol) and 6 (1.78 kcal/mol). Thus, it seems the intensity of VCD correlates with relative energies (enthalpies; in kcal/mol) of individual forms. On the other hand, the stability of a crystal form is influenced by larger interaction networks as partially documented by **Table S3** in SI, where we tried to estimate elongation energy for all forms using a simplified model. The elongation energy corresponds to the elongation of a crystal (represented by a single unit cell) by additional unit cell in a certain direction (a, b, and c; see schematic explanation in **Table S3**). Here we will discuss only the lowest $E_{\text{elongation}}$ energies for each form that always corresponded to interactions of molecules of the stacks. When we compare these numbers for all forms, we observe the lowest $E_{\text{elongation}}$ for form 6 (-24.5 kcal/mol = -102.6 kJ/mol) closely followed by form 7 (-23.4 kcal/mol = -97.9 kJ/mol). The energy for form 1 was substantially higher (-20.3 kcal/mol = -85.0 kJ/mol). This trend agrees with conclusions on stability reported before.[26] In addition, the reported interaction energies[26] (for molecules of the stacks) of -72.9, -109.6, and -101.6 kJ/mol are in good agreement with our observed $E_{\text{elongation}}$. Thus, our calculations might indicate a relatively local environmental impact on the solid-state VCD rather than an effect of any long-range interactions.

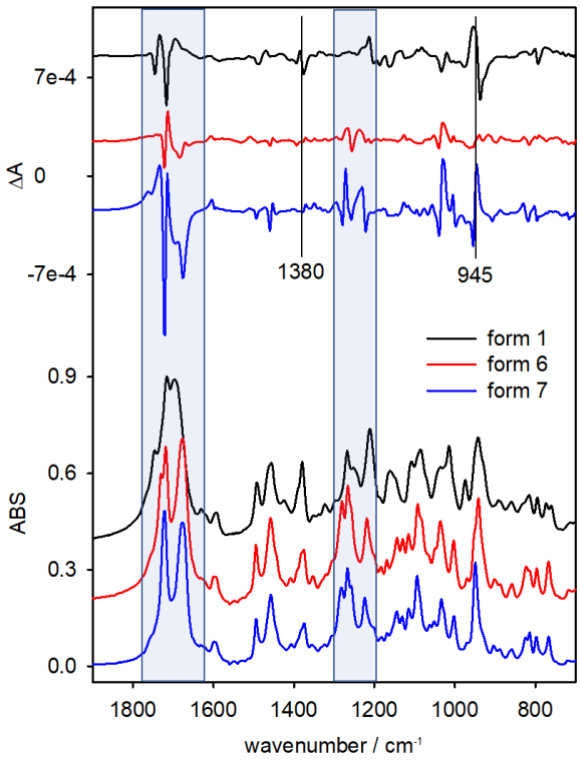

Figure 11. ssVCD (top) and IR (bottom) spectra of three polymorphs of sofosbuvir in KBr matrix (20 mm diameter pellets, 6 scanning blocks).

4. Discussion

In the previous sections, we have presented and revealed the advantages and disadvantages of two alternative approaches used in sample preparation for the subsequent VCD experiment of solid samples. This involves mixing the analyte with an inert matrix and pressing it into a pellet, and preparing a sample suspension in mineral oil. In terms of method optimization, we have investigated the effect of different experimental conditions on the quality of spectra.

The most convenient experimental approach for measuring solid-state VCD spectra is to prepare a KBr pellet large enough in diameter to cover the whole cross-section of the incident beam of infrared circularly polarized light. Nevertheless, even a pellet twice as small, which deprives us of a significant part of the light, can provide qualitatively well-structured spectra in the range 1800-1000 cm^{-1}. The mulling technique is also applicable; however, the absorption of mulling agents and a considerably laborious preparation of the sample make this possibility not advantageous.

According to our results, an hour-long spectral recording represents a minimum to obtain a satisfactory spectrum, however, a three-hour recording is preferable and provides us with a good-quality and reproducible spectrum. Although, this may be a system-dependent issue, 1-3 hours experiments provided qualitatively good spectra for all solid-state samples studied in this work (alanine, serine, tyrosine, tartaric acid, and sofosbuvir).

In case of the tested samples, the method of grinding an analyte turned out to be unimportant because the resulting sizes of particles of all tested compounds were comparable. Nevertheless, we cannot rule out the possibility that for some crystals the grinding method may be essential. We showed the necessity of averaging multiple orientations due to the anisotropic occurrence of the solid phase. It is always preferable to rotate the sample holder to eliminate the anisotropy of the sample.

By measuring other acids besides alanine, we confirmed the reliability and robustness of the experimental approach. In the case of alanine and serine, we achieved even better spectra compared to data published before.[18, 37] Furthermore, our approach for ssVCD was applied for a wider region of wavenumbers (2000 – 800 cm^{-1}) than published before.[18, 37] The amino- and hydroxy acids are, however, quite small and the conformations of each are similar. To test the universality of our approach, larger molecules with energetically distant conformers and more polymorphs should be tested. We also expect that slight modification (different concentration at least) of the approach is necessary for ssVCD in the CH stretching region.

The ssVCD analysis of the antiviral drug sofosbuvir proved that polymorphs can be well and unmistakably distinguished using ssVCD. The validation of our optimized methodology revealed trends in the relationship between spectral pattern and crystal structure. Based on the well-described crystal structure and stability of all three polymorphs, we conclude that the spectral patterns remain similar when the molecules in the crystal lattice are conformationally similar; this applies to forms 6 and 7. On the other hand, the intensity of signals increases in the case of a specific space group. Both forms 1 and 7 crystallize in the $P2_1$ and exhibit higher VCD intensity, whereas form 6 with a different space group ($P2_12_12_1$) has rather low intensities of signals. Therefore, enhancement of VCD intensity of solids seems to be related to the symmetry of the crystal structure.

5. Conclusion

In this work, we designed an optimal approach to obtain reliable VCD spectra of solid-state samples in the region of 2000-800 cm^{-1}. We assessed the effect of various experimental conditions on resulting spectra of selected crystalline acids. Thus, we suggest that a three-hour-long experiments performed for a sample in a 20 mm pellet provide high-quality and reproducible spectra. Nevertheless, most spectral features can be obtained even within an hour for a 7 mm pellet prepared using a simple table press. Different alkali halides (KBr, KCl, CsI) used as the matrix pellet material cause only minor changes. Samples prepared using mineral oils provide comparable VCD spectra as pellets, however their utilization is more elaborate, therefore the pellet-based approach is recommended. The effect of sample grinding on recorded VCD was negligible. Using presented optimized approach, we acquired almost perfect mirror image spectra of enantiomers of alanine, serine, tyrosine, and tartaric acid. Furthermore, we successfully distinguished three polymorphs of sofosbuvir using ssVCD. The DFT calculations helped us to decipher observed differences in experimental spectra. We conclude that conformational polymorphism of sofosbuvir results in significant spectral differences, while different spatial symmetry of a crystal lattice influences rather the signal intensities.

Thus, we demonstrate that solid-state VCD is a promising alternative method for solid-state analysis that can broaden the portfolio of standard solid-state methods. Although simple XRPD phase analysis can be performed in tens of minutes, VCD still can be valuable as it is sensitive to chirality and provides additional structural information. This chiral variant of vibrational spectroscopy is very sensitive to weak molecular interactions, and as we demonstrated on sofosbuvir could detect differences between polymorph structures. Contrary to X-ray, it provides global information on a macroscopic sample. Therefore, it represents a great potential in many scientific and commercial fields and should find its application in pharmaceutical research and development.

Acknowledgments

The Czech Ministry of Education, Youth and Sports (Grant LTAUSA18085) are gratefully acknowledged. Computational resources were supplied by the project "e-Infrastruktura CZ" (e-INFRA CZ LM2018140) supported by the Ministry of Education, Youth and Sports of the Czech Republic. Jakub Kaminský also acknowledges the European Regional Development Fund OP RDE (Project ChemBio-Drug, Grant CZ.02.1.01/0.0/0.0/16_019/0000729) for the support and computational resources.

Author contributions

Adam Sklenář – Investigation, Methodology, Visualization, Writing - original draft; Lucie Růžičková – Investigation, Writing - review & editing; Lucie Bednárová – Supervision, Writing - review & editing; Markéta Pazderková – Conceptualization, Writing - review & editing; Argyro Chatziadi - Investigation; Eliška Skořepová – Supervision, Writing - review & editing; Miroslav Šoóš - Supervision, Writing - review & editing; Jakub Kaminský – Conceptualization, Resources, Project administration, Supervision, Writing - review & editing

Supplementary data

Supplementary data to this article can be found online at:

Declaration of competing interest

The authors declare that they have no known competing financial interests or personal relationships that could have appeared to influence the work reported in this paper.

References

[1] I. Sathisaran, S.V. Dalvi, Engineering Cocrystals of PoorlyWater-Soluble Drugs to Enhance Dissolution in Aqueous Medium, Pharmaceutics, 10 (2018) 108.
[2] K. Kubota, S. Kumakura, Y. Yoda, K. Kuroki, S. Komaba, Electrochemistry and solid-state chemistry of NaMeO2 (Me= 3d transition metals), Adv. Energy Mater., 8 (2018) 1703415.
[3] J. Frelek, M. Gorecki, A. Dziedzic, E. Jablonska, B. Kamienski, R. K. Wojcieszczyk, R. Luboradzki, W. J. Szczepek, Comprehensive spectroscopic characterization of finasteride polymorphic forms. Does the form X exist?, J. Pharm. Sci., 104 (2015) 1650-1657.
[4] A. J. Cruz-Cabeza, M. Lestari, M. Lusi, Cocrystals Help Break the “Rules” of Isostructurality: Solid Solutions and Polymorphism in the Malic/Tartaric Acid System, Cryst. Growth Des., 18 (2017) 855-863.
[5] P. J. Hasnip, K. Refson, M. I. J. Probert, J. R. Yates, S. J. Clark, C. J. Pickard, Density functional theory in the solid state, Phil. Trans. R. Soc. A, 372 (2014) 20130270.

[6] V. Štejfa, A. Bazyleva, M. Fulem, J. Rohlíček, E. Skořepová, K. Růžička, A. V. Blokhin, Polymorphism and thermophysical properties of L-and DL-menthol, The Journal of chemical thermodynamics, 131 (2019) 524-543.
[7] A. W. Newman, S. R. Byrn, Solid-state analysis of the active pharmaceutical ingredient in drug products. , Drug Discov. Today, 8 (2003) 898–905.
[8] R. K. Chandrappa, P. Ochsenbein, C. Martineau, M. Bonin, G. Althoff, F. Engelke, H. Malandrini, B. Castro, M. El Hajji, F. Taulelle, Polymorphism in Xaliproden (SR57746A): An X-ray Diffraction, Calorimetric, and Solid-State NMR Investigation, Cryst. Growth Des., 13 (2013) 4678–4687.
[9] A. Rakhmatullin, M. Allix, I.B. Polovov, D. Maltsev, A.V. Chukin, R. Bakirov, C. Bessada, Combining solid state NMR, powder X-ray diffraction, and DFT calculations for $CsSc_3F_{10}$ structure determination., J. Alloys Compd., 787 (2019) 1349-1355.
[10] S. Bates, G. Zografi, D. Engers, K. Morris, K. Crowley, A. Newman, Analysis of Amorphous and Nanocrystalline Solids from Their X-Ray Diffraction Patterns, Pharm. Res., 23 (2006) 2333–2349.
[11] X. Chen, M.L. Clarke, J. Wang, Z. Chen, Sum Frequency Generation Vibrational Spectroscopy Studies on Molecular Conformation and Orientation of Biological Molecules at Interfaces, Int. J. Mod. Phys. B., 19 (2005) 691-713.
[12] S. Krimm, J. Bandekar, Vibrational spectroscopy and conformation of peptides, polypeptides, and proteins, Adv. Protein Chem. , 38 (1986) 181-364.
[13] H. Matsuura, K. Fukuhara, Vibrational spectroscopic studies of conformation of poly (oxyethylene). II. Conformation–spectrum correlations. , J. Polym. Sci. B Polym. Phys., 24 (1986) 1383-1400.
[14] M. Donahue, E. Botonjic-Sehic, D. Wells, C.W. Brown, Understanding infrared and Raman spectra of pharmaceutical polymorphs, Am. Pharm. Rev., 14 (2011) 104-110.
[15] A. Heinz, C.J. Strachan, K. C. Gordon, T. Rades, Analysis of solid-state transformations of pharmaceutical compounds using vibrational spectroscopy, J. Pharm. Pharmacol., 61 (2009) 971-988.
[16] T. Kuppens, P. Bultinck, W. Langenaeker, Determination of absolute configuration via vibrational circular dichroism. , Drug Discov. Today Technol., 1 (2004) 269-275.
[17] N. Jiang, R. X. Tan, J. Ma, Simulations of solid-state vibrational circular dichroism spectroscopy of (S)-alternarlactam by using fragmentation quantum chemical calculations, J. Phys. Chem. B, 115 (2011) 2801-2813.
[18] I. Kawamura, H. Sato, Solid-state vibrational circular dichroism studies of L- and D-serine, Anal. Biochem., 580 (2019) 14-20.
[19] H. Sato, A new horizon for vibrational circular dichroism spectroscopy: a challenge for supramolecular chirality, Phys. Chem. Chem. Phys., 22 (2020) 7671-7679.
[20] V. Declerck, A. Perez-Mellor, R. Guillot, D.J. Aitken, M. Mons, A. Zehnacker, Vibrational circular dichroism as a probe of solid-state organisation of derivatives of cyclic beta-amino acids: Cis- and trans-2-aminocyclobutane-1-carboxylic acid, Chirality, 31 (2019) 547-560.
[21] M. S. Møller, M. C. Liljedahl, V. McKee, C. J. McKenzie, Solid Phase Nitrosylation of Enantiomeric Cobalt(II) Complexes, Chemistry, 3 (2021).
[22] J. Frelek, M. Gorecki, M. Laszcz, A. Suszczynska, E. Vass, W.J. Szczepek, Distinguishing between polymorphic forms of linezolid by solid-phase electronic and vibrational circular dichroism, Chem. Commun., 48 (2012) 5295-5297.
[23] P. Rizzo, M. Beltrani, G. Guerra, Induced vibrational circular dichroism and polymorphism of syndiotactic polystyrene, Chirality, 22 Suppl 1 (2010) E67-73.

[24] R. Kuroda, T. Harada, Y. Shindo, A solid-state dedicated circular dichroism spectrophotometer: Development and application., Rev. Sci. Instrum. , 72 (2001) 3802-3810.
[25] N. Berova, P.L. Polavarapu, K. Nakanishi, R. W. Woody, Comprehensive chiroptical spectroscopy: applications in stereochemical analysis of synthetic compounds, natural products, and biomolecules, John Wiley & Sons2012.
[26] A. Chatziadi, E.k. Skořepová, J. Rohlíček, M. Dušek, L.k. Ridvan, M. Šoóš, Mechanochemically Induced Polymorphic Transformations of Sofosbuvir, Crystal Growth & Design, 20 (2019) 139-147.
[27] M.-H. Qi, M.-H. Hong, Y. Liu, E.-F. Wang, F.-Z. Ren, G.-B. Ren, Estimating Thermodynamic Stability Relationship of Polymorphs of Sofosbuvir, Crystal Growth & Design, 15 (2015) 5062-5067.
[28] J. P. Perdew, K. Burke, M. Ernzerhof, Generalized gradient approximation made simple., Phys. Rev. Lett. , 77 (1996) 3865.
[29] S. Grimme, Semiempirical GGA-type density functional constructed with a long-range dispersion correction., J. Comput. Chem. , 27 (2006) 1787-1799.
[30] H. J. Monkhorst, J. D. Pack, Special points for Brillouin-zone integrations., Phys. Rev. B 13 (1976) 5188.
[31] A. D. Bochevarov, E. Harder, T. F. Hughes, J. R. Greenwood, D. A. Braden, D. M. Philipp, D. Rinaldo, M. D. Halls, J. Zhang, R. A. Friesner, Jaguar: A high-performance quantum chemistry software program with strengths in life and materials sciences., Int. J. Quantum Chem., 113 (2013) 2110-2142.
[32] P. R. Spackman, M. J. Turner, J. J. McKinnon, S. K. Wolff, D. J. Grimwood, D. Jayatilaka, M. A. Spackman, CrystalExplorer: A program for Hirshfeld surface analysis, visualization and quantitative analysis of molecular crystals., J. Appl. Crystallogr. , 54 (2021) 1006-1011.
[33] E. Castiglioni, P. Biscarini, S. Abbate, Experimental aspects of solid state circular dichroism, Chirality: The Pharmacological, Biological, and Chemical Consequences of Molecular Asymmetry, 21 (2009) E28-E36.
[34] M. Hirschmann, C. Merten, C. M. Thiele, Treating anisotropic artefacts in circular dichroism spectroscopy enables investigation of lyotropic liquid crystalline polyaspartate solutions, Soft Matter, 17 (2021) 2849-2856.
[35] M. Diem, E. Photos, H. Khouri, L. A. Nafie, Vibrational circular dichroism in amino acids and peptides. 3. Solution-and solid-phase spectra of alanine and serine, J. Am. Chem. Soc., 101 (1979) 6829-6837.
[36] H. Sato, I. Kawamura, Solid-state vibrational circular dichroism studies on the conformation of an amino acid molecule in crystalline state, Biochim. Biophys. Acta Proteins Proteom., 1868 (2020) 140439.
[37] S. Jahnigen, A. Scherrer, R. Vuilleumier, D. Sebastiani, Chiral Crystal Packing Induces Enhancement of Vibrational Circular Dichroism, Angew. Chem. Int. Ed., 57 (2018) 13344 –13348.